PCCP

Accepted Manuscript

ROYAL SOCIETY OF CHEMISTRY

www.rsc.org/pccp

Journal Name

ARTICLE TYPE

Cite this: DOI: 10.1039/xxxxxxxxxx

Investigating the properties of PODIPY (Phosphorous-Dipyrromethene) with *ab initio tools*†

Arnaud Fihey,[a] Anthony Favennec,[a] Boris Le Guennic*[b] and Denis Jacquemin*[a,c]

Received Date
Accepted Date

DOI: 10.1039/xxxxxxxxxx

www.rsc.org/journalname

We investigate with a hybrid SOS-CIS(D)/TD-DFT approach accounting for solvation effects, the structural, electronic and optical properties of recently-proposed PODIPY dyes. Being more soluble in water than the well-known BODIPYs, these new chromogens are particularly appealing, but their characterization remains very limited. It turns out that the selected theoretical protocol could reproduce the experimentally reported differences between PODIPY and BODIPY dyes. On this basis, we have investigated a large number of new PODIPY dyes and determined their theoretical 0-0 energies.

1 Introduction

Among the existing near-infrared dyes, boron-dipyrromethene (BODIPY) and their aza-derivatives (aza-BODIPY) certainly occupy privileged spots (see Figure 1). Indeed, these fluoroborate compounds display remarkable properties: extremely large molar absorption coefficients, large fluorescence quantum yields (up to 0.99), easily tunable absorption and emission wavelengths and interesting photostabilities in both solution and solid state.[1–4] The exceptional optical properties of (aza-)BODIPY can be traced back to their electronic structure: these compounds can indeed be viewed as *cis*-constrained cyanines. However, most BODIPY are very poorly soluble in water, which impedes straightforward bio-applications. This is why several strategies have been applied to make BODIPY more soluble, e.g., through the addition of sulfonate groups.[5–10] Very recently, Jiang and coworkers have proposed an alternative strategy to improve the water solubility: they replaced the BF_2 unit of the dyes by a PO_2 group (see Figure 1).[11] Indeed, by treating the (aza-)dipyrromethene with $POCl_3$ in presence of ET_3N, they could obtain, after hydrolysis, one PODIPY (**1-PO2**) and one aza-PODIPY (**2-PO2**). **1-PO2** shows a good solubility in water (13 mg.L^{-1}), and can remain in solution for at least two weeks.[11] These two phosphorous-containg molecules constitute the first members of a new sub-family of cyanine derivatives. These new dyes present an absorption band that is slightly redshifted compared to the corresponding fluroborate (e.g., -15 nm when going from **2-BF2** to **2-PO2**) and also develop slightly larger Stokes shifts (e.g., 871 cm^{-1} for **2-PO2** *versus* 496 cm^{-1} for **2-BF2**). Apart from the HOMO-LUMO plots presented in the original work (B3LYP level),[11] there is, to the best of our knowledge, no attempt to rationalize and predict the properties of PODIPY with theoretical tools, and the present contribution aims to fill this gap.

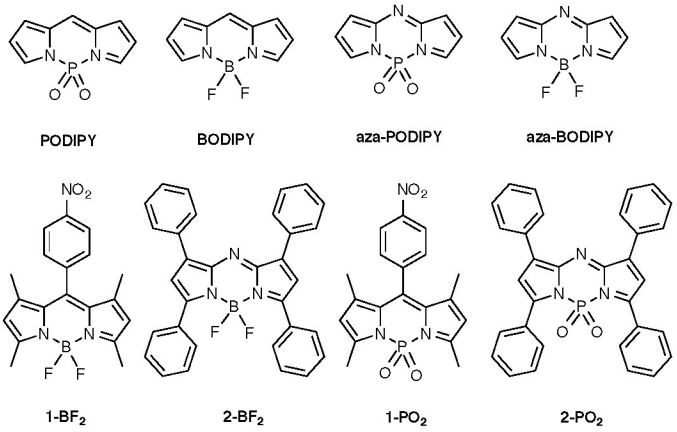

Fig. 1 Top: Representation of the chromogens for the family of compounds investigated here. To designate these specific structures, bold names are used in the text to distinguish them from the generic family names. Bottom: synthesized PODIPY (**1-PO2**) and aza-PODIPY (**2-PO2**)[11] a s well as the corresponding fluoroborate structures, BODIPY (**1-BF2**) and aza-BODIPY (**2-BF2**).

The simulation of the excited-state properties of dyes with theoretical tools remains an important challenge.[12] In the present investigation, three difficulties have to be overcome. Firstly, as we wish to model the positions and topologies of both the absorption

[a] *Chimie Et Interdisciplinarité, Synthèse, Analyse, Modélisation (CEISAM), UMR CNRS no. 6230, BP 92208, Université de Nantes, 2, Rue de la Houssinière, 44322 Nantes, Cedex 3, France; E-mail: Denis.Jacquemin@univ-nantes.fr*

[b] *Institut des Sciences Chimiques de Rennes, UMR 6226 CNRS-Université de Rennes 1, 263 Av. du Général Leclerc, 35042 Rennes Cedex, France; E-mail: Boris.leguennic@univ-rennes1.fr*

[c] *Institut Universitaire de France, 103 bd St. Michel, 75005 Paris Cedex 5, France*

† Electronic Supplementary Information (ESI) available: representation of the key coupling vibronic modes, representation of water complexes. See DOI: 10.1039/b000000x/

and emission bands, vibronic couplings have to be determined. However, the calculation of these couplings generally requires the computation of the Hessian of the excited-state, a demanding task that can, in practice, only be tackled with Time-Dependent Density Functional Theory (TD-DFT)[13–15] for the compounds investigated in this work. As a reward of this computational effort, the difference between the zero point vibrational energies of the ground and excited states can be calculated, which, in turn gives a direct access to the absorption-fluorescence crossing points (AFCP).[16,17] Like the band shapes, the AFCP energies can be directly compared to the experiment on a solid physical basis. Secondly, solvent effects have to be accounted for, and we have recently showed that only refined environmental models are suitable for BODIPY structures.[18] In other words simple "linear-response" solvation schemes are inadequate because they strongly overshoot solvatochromic effects. Thirdly, the treated systems belong to the cyanine class of dyes. It is well-documented that the transition energies of such derivatives are particularly difficult to reproduce due to large differential electron correlation effects between the ground and the excited states.[19–23] For this reason, (the common adiabatic formulation of) TD-DFT is not appropriate to determine absorption and emission wavelengths and, in practice, it is mandatory to select a method explicitly including contributions from double excitations to reach accurate results. However, such methods imply a strong increase of the computational cost compared to TD-DFT, especially if the vibrational signatures of the excited states are to be computed. For this reason, we apply here a mixed protocol: the geometries and vibrational levels are computed with TD-DFT, the solvent effects are modeled with the cLR approach, whereas the transition energies are determined with an approach accounting for double excitations (see next Section). This approach was successfully used to reproduce the band positions and shapes in several BODIPY derivatives.[24–26]

This paper is divided as follows. In the next Section, we summarize the selected theoretical approach. In Section 3 we discuss our results starting by an in-depth characterization of the compounds displayed in Figure 1, followed by a screening of a large set of compounds. This second step aims to provide insights into the (statistical) differences between fluoroborates and their phosphorus counterparts. We conclude in Section 4.

2 Computational Details

As stated above, while the structures of cyanine-like dyes can be obtained with TD-DFT, approaches accounting for contributions from double excitations have to be applied to reach reliable total and transition energies.[23,27] This is why we designed a specific hybrid protocol for cyanine-like dyes that uses the M06-2X hybrid functional[28] for computing the geometries and vibrational signatures of both the ground and the excited-states while the SOS-CIS(D) (Scaled-Opposite-Spin Configuration Interaction Singles with a perturbative Double correction) approach[29,30] is applied to determine the absorption, emission and adiabatic energies of all investigated compounds.[23] Once coupled to an advanced variation of the Polarizable Continuum Model (PCM),[31] e.g., the corrected linear-response approach (cLR),[32] this protocol delivers accurate AFCP energies for various classes of BODIPY derivatives.[24–26] As this protocol was detailed previously, we only summarize it below.

DFT and TD-DFT (M06-2X) calculations were carried out with the latest version of the Gaussian09 program package,[33] applying both a tightened self-consistent field convergence criterion ($10^{-9}-10^{-10}$ au) and an improved optimization threshold (10^{-5} au on average residual forces). For each compound, we have optimized the geometry of both the ground and the first excited states, as well as computed the (harmonic) vibrational spectra of both states, using the default procedure implemented in Gaussian09. The same DFT integration grid, namely the so-called *ultrafine* pruned (99,590) grid, was used for both the ground and excited states. Except in Section 3.1 where solvent-phase structures are used, these structural and vibrational parameters have been determined in gas-phase using the 6-31G(d) atomic basis that was previously showed to be sufficient for BODIPY derivatives.[34] In Section 3.1, we used the equilibrium solvation limit for the optimizations. The total and transition energies were determined with a much larger basis set, namely 6-311+G(2d,p), a choice justified by previous benchmarks.[34,35] These energies have been first determined with DFT and TD-DFT both in gas-phase and in condensed phase (dicholoromethane, as in the experiments).[11] For rationalization purposes, the same solvent was used to screen the optical properties of our series of new PODIPYs. For the TD-DFT step, the cLR-PCM approach was used to model the solvent.[32] In Section 3.2, the solvation energies have been computed at the SMD level implemented in Gaussian09.[36,37] In the same Section, the complexation energies with water molecules have been obtained by taking into account the Basis Set Superposition Error (BSSE), in gas phase, at the M062X/6-311+G(2d,p) level of theory. The SOS-MP2 and SOS-CIS(D) energies were determined with the *Q-Chem* package using the Resolution of the Identity (RI) scheme and the 6-311+G(2d,p) atomic basis set.[38] Theoretical best estimates of the AFCP energies can be obtained by correcting the condensed phase TD-DFT results by the difference between the TD-DFT and SOS-CIS(D) adiabatic energies computed in gas-phase. We redirect the reader to Ref. 23 and references therein for more details.

Vibrationally resolved spectra within the harmonic approximation were computed using the FCclasses program (FC)[39–42] on the basis of TD-DFT harmonic vibrational signatures determined in solution (optimization and vibrations computed taking into account PCM in the equilibrium limit). The reported spectra were simulated using a convoluting Gaussian function presenting a half width at half maximum (HWHM) that was adjusted to allow direct comparisons with experiments (typical value: 0.04 eV). A maximal number of 25 overtones for each mode and 20 combination bands on each pair of modes were included in the calculation. The maximum number of integrals to be computed for each class was first set to 10^6. In the cases where convergence of the FC factor [≥ 0.9] could not be achieved with this number of integrals, a larger value (10^{12}) was used so to go over the 0.9 limit.

3 Results and discussion

3.1 Comparison of BODIPY and PODIPY chromogens

We first focus on the description of the impact of the replacement of the BF_2 group by the PO_2 moiety considering the chromophores represented at the top of Figure 1. A first obvious geometrical difference can be found. Indeed, due to its size, the phosphorous atom lies more strongly out of the plane formed by the π-conjugated skeleton than the boron atom (see also the ESI). In Table 1 we list the AFCP energies determined by the above-described protocol, together with the ground-state dipole moments for these four model structures. As stated previously, our protocol has been successfully validated for a large variety of BODIPY dyes and both the standard deviation and mean absolute error were found smaller than 0.1 eV,[24] and the E^{AFCP} presented in Table 1 can therefore be trusted.

Table 1 AFCP energies (in eV) and ground-state dipole moments (in D) determined for the model compounds.

	E^{AFCP} (eV)	μ^{GS} (D)
BODIPY	2.36	5.56
PODIPY	2.34	9.75
aza-BODIPY	2.11	2.67
aza-PODIPY	2.08	7.04

For **BODIPY** and **PODIPY**, the AFCP energies are 2.36 and 2.34 eV, respectively, indicating that the presence of the PO_2 group induces a slight redshift of 0.02 eV (5 nm). For the corresponding aza-fluorophores, a similar shift of 0.03 eV (7 nm) can be calculated. These variations, in line with the experimental trends,[11] remain significantly smaller than the typical spectral differences between dipyrromethenes and aza-dipyrromethenes,[1] that our approach reproduces as well.[3] By investigating the TD-DFT vertical absorption and emission energies, it appears that the change of E^{AFCP} induced by the PO_2 group can be mostly ascribed to a variation of the fluorescence energy (-0.09 eV between **BODIPY** and **PODIPY**), the absorption being significantly less affected (-0.01 eV). The same holds for the aza-dyes.

For all four fluorophores of Table 1 the electronic transition of interest corresponds, as expected, to a $\pi \rightarrow \pi^\star$ HOMO→LUMO transition not significantly involving the BF_2 or PO_2 groups (see Figure 2). The small variations of AFCP energies discussed above is therefore not related to a significant variation of the topology of the molecular orbitals, but more to a change of their relative energies, e.g., going from **BODIPY** to **PODIPY** induces a downshift of the HOMO and LUMO by -0.44 eV and -0.41 eV, respectively. This effect can be ascribed to stronger electron-withdrawing character of the PO_2 group, that is to the different charge distribution (see next Section). From the theoretical viewpoint, we therefore note that the DFT gap determined in **PODIPY** (4.93 eV) is therefore smaller than in **BODIPY** (4.90 eV), which, in a first crude approximation, indicates a qualitatively incorrect spectral shift compared to experiment.[11] In contrast, as seen above, TD-DFT that accounts for relaxation effects does reproduce the correct trend.

As stated in the Introduction, BODIPY derivatives are often characterized by hallmark band shapes (for both absorption and emission spectra): a sharp peak is accompanied by a shoulder.[1,2,43] For this reason, we have determined vibronic couplings and subsequently obtained vibrationally-resolved spectra for the four model chromophores. The results are displayed in Figure 3 and the presence of a shoulder is nicely reproduced, though its relative height compared to experiment is overestimated (but, to a lesser extend for **aza-BODIPY**), a trend consistent with previous TD-DFT simulations of fluoroborates.[3,34] We underline that Figure 3 clearly shows that the Stokes shifts are larger for the **(aza)-PODIPY** dyes than for their fluoroborates counterparts, e.g., the Stokes shift attains 0.07 eV for **PODIPY** but 0.02 eV for **BODIPY**, a trend, well in the line of experimental measurements.[11] We also notice that while the spectra of **BODIPY** and **aza-BODIPY** are noticeably different, **PODIPY** and **aza-PODIPY** present similar spectra except for the expected redshift.[1,44] We have investigated the nature of the vibrational modes principally responsible for the observed band shape. It turned out that, in all compounds, a low-energy vibration, presenting a similar nature in both the ground and excited states, explains the broadening of the main (0-0) band. This mode corresponds to out-of-plane deformations with the movement of the BF_2/PO_2 moiety being in opposite phase from the rest of the molecule. It is is sketched in Figure ESI-1 in the ESI. The presence of a shoulder is explained by vibronic couplings involving several vibrational modes, that are depicted in Figure ESI-2 in the ESI. For the absorption, one dominant mode, corresponding to a breathing of the central six-member cycle, explains the shoulder for both **PODIPY** (729 cm^{-1}) and **aza-PODIPY** (762 cm^{-1}). In contrast additional modes are involved in **BODIPY** and **aza-BODIPY** (see the ESI). Interestingly, a significant difference of nature was found between **(aza-)BODIPY** and **(aza-)PODIPY**. Indeed, in the latter dyes the vibronic contributions implying these high-energy vibration also contain a strong coupling with the low-energy vibration mentioned above, that is, they are combinations of two vibrations, which contrasts with the former compounds, that present significant single-mode contributions even for high-energy modes. This can explain the broader bands in **PODIPY** compared to **BODIPY**: it is clear that the systematic combination with the first mode for the PO_2 chromogens, more than the proper nature of the vibration themselves is the origin of the different band shapes. In addition, this combination washes out the difference between the nitrogen- and carbon-based structures, i.e., the band shapes of **BODIPY** and **aza-BODIPY** differ more strongly from one another[1,44] than their **PODIPY** and **aza-PODIPY** counterparts.

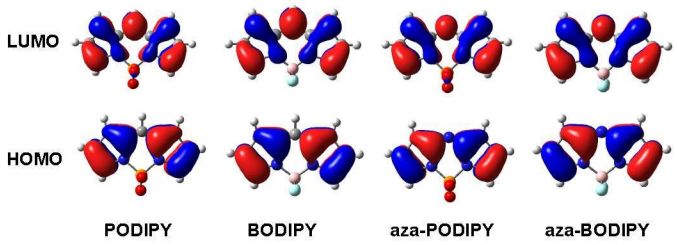

Fig. 2 Frontier molecular orbitals for the model chromogens (cut-off = 0.03 a.u.).

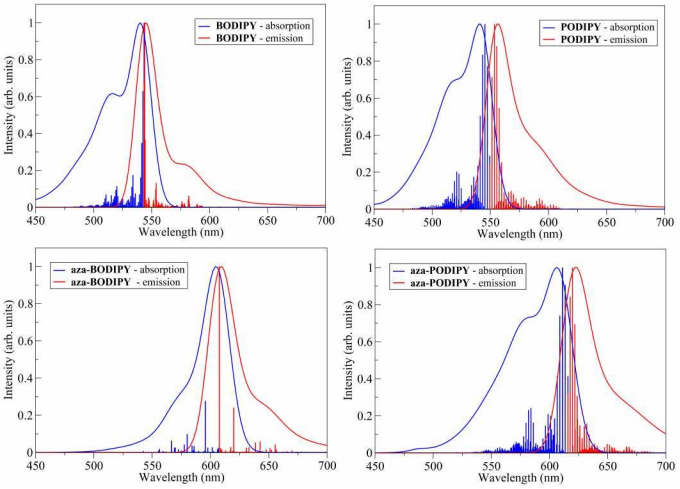

Fig. 3 Theoretical vibrationally-resolved spectra for the four model chromogens: blue: absorption, red: emission. In both cases, both the individual vibronic contributions and the convoluted spectra are reported.

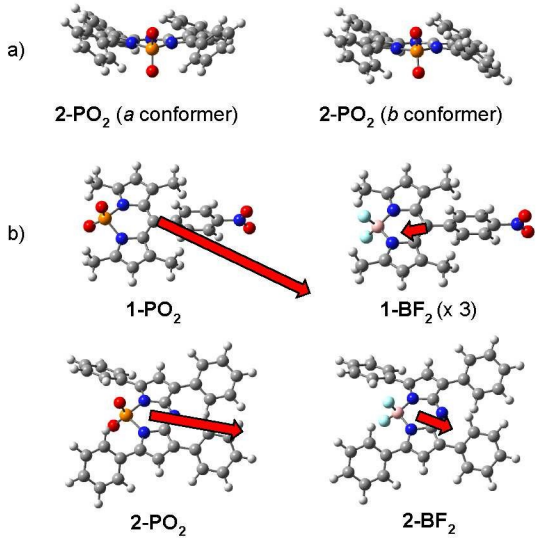

Fig. 4 Top (a): two conformers for **2-PO$_2$**. Bottom (b): orientation and (relative) magnitude of the ground-state dipole moment for the experimentally available compounds sketched in Figure 1. For **1-BF$_2$**, the total dipole has been scaled by a factor of three to allow its representation.

3.2 Synthesized compounds

3.2.1 Solubility with water

As stated in the Introduction, fluorphores **1-PO$_2$** and **2-PO$_2$**, depicted in Figure 1 have been recently designed with the primary goal of improving the solubility in water,[11] and it was indeed observed experimentally for both compounds. To rationalize this finding, we have considered three aspects: i) the relative dipole moments in the two series of compounds, ii) their solvation energies as obtained from SMD calculations; and iii) the strengths of the H-bonds in dye-water complexes. First, we note that for both **2-BF$_2$** and **2-PO$_2$**, two thermodynamically stable conformers differing by the relative orientations of the phenyl rings can be designed. They are represented in Figure 4. Although the *a* conformation is systematically favored, the Gibbs energy differences computed for the two conformers are trifling: 0.08 kcal.mol^{-1} for **2**-PO$_2$ and 0.62 kcal.mol^{-1} for **2**-BF$_2$. As the two conformers display very similar spectral properties, we continue in the following with the most stable *a* conformer only.

Table 2 lists the (MK) partial atomic charges of selected atoms as well as the total dipole moments for **1-PO$_2$**, **1-BF$_2$**, **2-PO$_2$** and **2-BF$_2$**. Overall, the negative charge borne by the oxygen atoms is ca. 0.2 $|e|$ larger (in absolute terms) than the corresponding value for fluorine atoms. As the phosphorous atoms are also more positively charged than the boron atoms, the charge separation is obviously increased in PODIPY. As underlined in Ref. 11, this improved separation can be intuited by an analysis of the Lewis structure, considering the *p* orbital of the phosphorous atom together with the lone pairs of the nitrogen atoms. As in the model chromophores, the global electric dipole moment (see Figure 4) is strongly affected by the nature of the heteroatom binding the dipyrromethene core: it increases by ca. 3–4 D when replacing boron by phosphorous. As a consequence, the magnitude of μ^{GS} is multiplied by a factor of 8.4 (2.7) when going from **1-BF$_2$** to **1-PO$_2$** (**2-BF$_2$** to **2-PO$_2$**), a trend clearly consistent with an improved solubility in polar solvents. This is confirmed by a calculation of the free solvation energies determined by comparing SMD(water) and gas phase energies (see Table 2) that also indicates a much larger stabilization of the PODIPY compared to the BODIPY.

Of course, the above approaches account for non-specific interactions only, and explicit solute-solvent interactions, notably H-bonds, are important for solubility in protic media. For this reason, we have also determined the complexes formed between one and two water molecules and the different fluorophores. The computed complexation energies are given in Table 2, while the structures are represented in Figure ESI-4 in the ESI. As expected, in all cases the most stable structures are obtained when the hydrogen atoms of the water molecules point toward the fluorine/oxygen atoms of the BF$_2$/PO$_2$ group to form H-bonds.[45] E^{comp} is almost perfectly doubled when going from one to two water molecules, and systematically more negative for the PO$_2$ derivatives than for the BF$_2$ counterparts. This systematic increase, that one can directly relate to the more negative partial charges borne by oxygen atoms than fluorine atoms (see Table 2), is far from negligible, e.g., E^{comp} increased from -15.93 kcal.mol^{-1} to -23.12 kcal.mol^{-1} when going from **2-BF$_2$** – 2 H$_2$O to **2-PO$_2$** – 2 H$_2$O. For the records, we note that there is no systematic relationship between E^{comp} and the H-bond lengths, e.g., the shortest H-bond length is 2.07 (2.13) Å in **1-BF$_2$** – H$_2$O (**1-PO$_2$** – H$_2$O), but 2.23 (2.12) Å in **2-BF$_2$** – H$_2$O (**2-PO$_2$** – H$_2$O). We also found that when going from one to two water molecules, the H-bond distances tend to decrease for all compounds.

In short, all theoretical results, i.e., charge-separation amplitude, dipolar nature, solvation energy and complexation energies, indicate that replacing BF$_2$ by PO$_2$ is favorable for solvation in water, a trend perfectly in the line of measurements.

Table 2 Merz-Kollman partial atomic charges (in $|e|$) for the key atoms in the dipyrromethene structure of the synthesized compounds, magnitude of the ground-state dipole moment (in D, determined in dichloromethane), water solvation energy obtained with the SMD model (in kcal.mol^{-1}) and complexation energies with one and two water molecules (in kcal.mol^{-1}).

	Partial atomic charges					Complexation energies	
Compound	B/P atoms	F/O atoms	N atoms	μ^{GS}	G^{solv}	E^{comp} (1 H_2O)	E^{comp}(2 H_2O)
1-PO$_2$	0.94	-0.67/-0.67	-0.26/-0.26	4.38	-18.81	-10.80	-21.61
1-BF$_2$	0.87	-0.45/-0.45	-0.34/-0.31	0.52	-7.01	-7.01	-14.78
2-PO$_2$	1.00	-0.66/-0.70	-0.22/-0.26	5.93	-19.49	-12.32	-23.12
2-BF$_2$	0.72	-0.46/-0.38	-0.27/-0.31	2.22	-9.48	-8.23	-15.93

3.2.2 Spectroscopic properties

Let us now turn to the optical properties of these compounds. As for the chromogens of Section 3.1, both the absorption and emission are solely involving transitions between the two frontier orbitals. They are displayed in Figure 5. First, we note that the HOMO and LUMO are spread symmetrically on both sides of the molecule, as expected for almost perfectly symmetric molecules. In other words, we do not retrieve the surprising B3LYP results of Jiang *et al.* that found the LUMO of the **2-PO$_2$** compound more localized on one side.[11] Globally, the shape of the frontier orbitals is the same for the BODIPY and PODIPY compounds, but for a small contribution of the *p*-nitro-phenyl group in the LUMO of **1-PO$_2$**. As can be seen in the density difference ($\Delta\rho$) plots (see Figure 5), the major impact of an electronic transition is a reorganization of the electron density on the chromophore and no significant charge-transfer takes place in these systems.

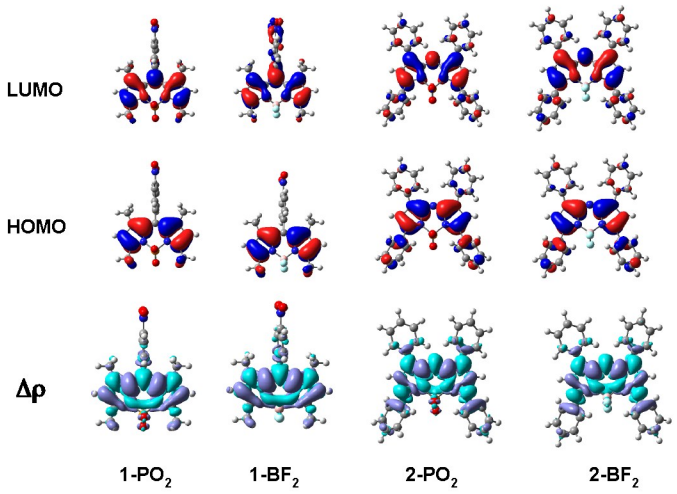

Fig. 5 Top and center: frontier molecular orbitals of (from left ro right) **1-PO$_2$**, **1-BF$_2$**, **2-PO$_2$** and **2-BF$_2$**. Bottom: difference of total density between the two states, $\Delta\rho$ for the same compounds. The cutoffs are 0.03 au for the MO and 0.0004 au for the density difference.

The computed spectroscopic data for **1** and **2** are listed in Table 3. Experimentally, the recorded absorption and emission wavelengths are respectively 510 nm and 524 nm for **1-PO$_2$**, and 625 nm and 661 nm for **2-PO$_2$**, in dichloromethane.[11] The measured corresponding AFCP energies are 2.40 eV and 1.93 eV. As can be seen in Table 3, TD-DFT AFCP energies are significantly too large, especially for **1-PO$_2$**. The SOS-CIS(D) corrected values are clearly more accurate but tends to undershoot the experimental values with errors of -0.16 and -0.23 eV for **1-PO$_2$** and **2-PO$_2$**, respectively. The variations with respect to the BF$_2$ derivatives are negligible with the SOS-CIS(D) scheme. Experimentally, a small bathochromic displacement of 15 nm (-0.05 eV) is found when going from **2-BF$_2$** to **2-PO$_2$**, and theory undershoots the magnitude of this change (-0.01 eV).

3.3 Screening of new derivatives

Given the potential importance of PODIPY and, because the experimental values are only available for two derivatives, we have decided to use theoretical chemistry as a screening tool for a larger number of PODIPY and aza-PODIPY derivatives (see Figure 6). Our goal was to determine if some compounds present particularly enhanced dipole moments compared to the fluoroborates (which would indicate enhanced solubility) or AFCP energies strongly evolving (ca. larger than 0.10 eV in absolute terms) when replacing BF$_2$ by PO$_2$. The results obtained in dichloromethane are given in Table 3

As can be seen in Figure 6, we have considered a vast panel of derivatives representative of various strategies (e.g., extension of the π-conjugation, stiffening of the lateral arms, addition of strongly active groups to induce charge-transfer, asymmetric N–O compounds...) used in the field. While the PODIPY and aza-PODIPY shown in Figure 6 are synthetically unknown compounds, they indeed all correspond to synthesized and characterized (aza-)BODIPY to ensure experimental access of the new compounds. For experimental characterizations of the fluoroborates, we redirect the interested reader to the original works: **3-BF2**,[46] **4-BF2**,[46] **5-BF2**,[47] **6-BF2**,[48] **7-BF2**,[48] **8-BF2**,[49] **9-BF2**,[50] **10-BF2**,[50] **11-BF2**,[49] **12-BF2**,[51] **13-BF2**,[52] **14-BF2**,[52] **15-BF2**,[53] **16-BF2**[54] and **17-BF2**.[55] For the dyes possessing side aromatic rings that can rotate (i. e, **3**, **4**, **6**, **7**, **8** and **11**), we considered the conformation *a* only (see Figure 4).

From Table 3, general tendencies regarding the impact of the substitution of the fluroborate center with a phosporous group can be drawn. First, it is clear that this substitution globally induces relatively limited variations of the AFCP energies for most compounds (smaller than 0.10 eV), regardless of the substitution pattern considered. As expected from the observations on the chromogens, we observe small redshifts for the majority of compounds, and in particular for all aza-BODIPYs considered in the present work. The situation seems slightly different for the BODIPYs treated here. Indeed, for **13**, **14**, **15**, **16** and **17** rather significant redshifts are obtained (-0.14, -0.11, -0.08, -0.17 and -0.16 eV, respectively), by both TD-DFT and SOS-CIS(D) methods.

Table 3 AFCP energies (TD-DFT with and without SOS-CIS(D) corrections) determined for the compounds of Figures 1 and 6 (eV). Ground-state dipole moments (D) for all compounds. All values determined using dichloromethane as solvent. At the right-hand-side of the Table the differences are reported to quantify the impact of the substitution of BF_2 by PO_2.

	(aza-)PODIPY, PO_2			(aza-)BODIPY, BF_2			Difference		
Compound	E^{AFCP}_{TD-DFT}	$E^{AFCP}_{SOS-CIS(D)}$	μ^{GS}	E^{AFCP}_{TD-DFT}	$E^{AFCP}_{SOS-CIS(D)}$	μ^{GS}	E^{AFCP}_{TD-DFT}	$E^{AFCP}_{SOS-CIS(D)}$	μ^{GS}
1	2.79	2.24	4.38	2.72	2.24	0.52	0.07	-0.00	3.86
2	2.10	1.70	5.93	2.10	1.71	2.22	-0.00	-0.01	3.71
3	2.07	1.68	9.92	2.07	1.68	6.17	-0.00	-0.00	3.75
4	1.98	1.57	6.00	2.00	1.60	3.58	-0.02	-0.03	2.42
5	1.81	1.51	4.03	1.87	1.57	5.97	-0.06	-0.06	-1.94
6	1.94	1.53	4.41	1.94	1.58	0.55	-0.00	-0.05	3.86
7	1.86	1.47	5.57	1.85	1.52	1.52	0.01	-0.05	4.05
8	1.78	1.36	2.42	1.80	1.41	1.15	-0.02	-0.05	1.27
9	1.96	1.57	6.25	1.99	1.60	2.85	-0.03	-0.03	3.40
10	1.88	1.43	4.87	1.92	1.51	1.08	-0.04	-0.08	3.79
11	1.87	1.41	2.90	1.91	1.45	4.24	-0.04	-0.04	-1.34
12	3.15	2.76	8.21	3.17	2.77	4.92	-0.02	-0.01	3.29
13	2.53	2.11	10.21	2.67	2.25	6.77	-0.14	-0.14	3.44
14	2.53	2.11	8.63	2.62	2.22	5.61	-0.09	-0.11	3.02
15	2.33	1.81	6.93	2.37	1.89	3.25	-0.04	-0.08	3.68
16	1.90	1.47	4.77	2.00	1.64	3.34	-0.10	-0.17	1.43
17	2.15	1.67	6.47	2.25	1.83	3.94	-0.10	-0.16	2.53

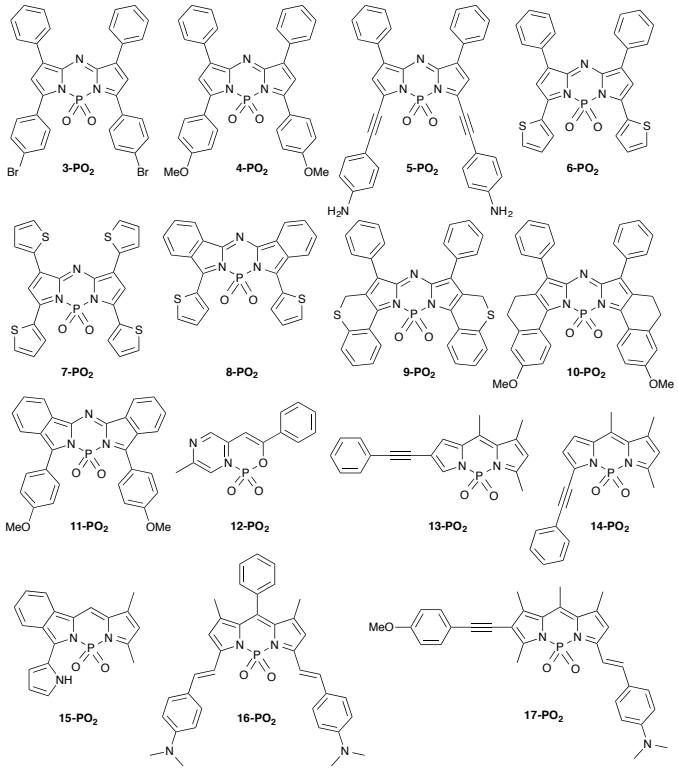

Fig. 6 Compounds used in the screening step. Only the PO_2 forms are shown.

The molecular orbitals involved in the excited state and the electronic density difference are given in Figure 7 for a symmetric aza-BODIPY (**8**) and an asymmetric BODIPY (**17**) compound. The HOMO and LUMO of the latter are principally localised one the arm bearing the NH_2 group, but are not visibly impacted when going from the PO_2 to the BF_2 derivatives, an outcome holding for **8** as well as for the $\Delta\rho$ plots. For all compounds, a closer investigation of the computed properties reveals that the emission energy is systematically more impacted by the incorporation of the PO_2 group than the absorption energy, which parallels what has been found for the model chromophores. For instance, **17**, that presents the largest redshift, has its emission energy decreased by 0.17 eV whereas its absorption is modified by 0.13 eV. This suggests that the Stokes shift is almost systematically larger in PODIPYs. From the comparison of the AFCP values of **16** and **17**, one can also note that symmetric and asymmetric BODIPYs can both undergo large redshifts. Interestingly, substituting a chelating nitrogen atom by an oxygen atom in the six-member ring (**12**) does not change the preceding trends, though the charge repartition in the PO_2 to the BF_2 groups is different.

Secondly, and regardless of the presence of BF_2 or PO_2, it is clear that increasing the π-conjugation length, induces smaller AFCP energies. This is why dyes with fused aromatic rings provide the most redshifted spectra in the series. Ultimately the incorporation of two thiophene rings in **8**, in addition to the fused benzopyrrole rings, yields the smallest AFCP energy of all systems investigated here: 1.36 eV and 1.41 eV for **8-PO$_2$** and **8-BF$_2$**, respectively, corresponding to a 33 nm redshift due to the phosphorous center. For these fluorophores the HOMO and LUMO are indeed delocalized on the whole π-system (see Figure 7).

Thirdly, while the dipole moment is, as expected, highly dependent on the structure of the fluorophore, the introduction of the PO_2 moiety clearly tends to increase its magnitude, typically doubling it. This hints to a superior solubility in polar sol-

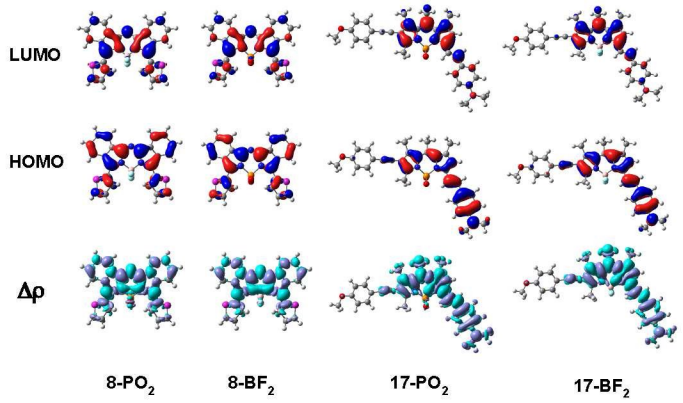

Fig. 7 Frontier molecular orbitals and electronic density difference for **8** and **17**. See caption of Figure 5 for more details.

vents of PODIPYs. In turn, this means that the benefits of using PODIPY instead of BODIPY for applications in water can probably be generalized to most of dipyrromethenes besides the two experimentally available. Exceptions were nevertheless found for two specific cases where strongly donating substituents are present, e.g., for **11** possessing OMe groups and **5** presenting NH_2 groups. This effect can be easily intuited as a counterbalance effect: the presence of the electroactive groups on this side of the molecule yielding an opposite effect to the PO_2 group. The corresponding dipole moments are displayed in the ESI for **5** and **11**. Nevertheless, the nature of the carbon-based conjugated skeleton (phenyls, fused rings) plays also a role in the charge distribution as other compounds also possessing methoxy groups, e.g., both **4** and **10** follow the general trend. In the considered series, the greatest dipole moment was obtained for **13-PO$_2$**.

4 Conclusions and outlook

Using state-of-the-art spectroscopic *ab initio* tools, we have investigated a brand-new class (only two synthesized compounds) of dipyrromethene derivatives, PODIPY, incorporating a phosphorous center and showing improved solubility in water. This particularity of PODIPYs, compared to the well-known BODIPYs, was rationalized using a series of complementary criteria. It was found that PODIPYs tend to present larger dipoles, larger solvation energies and increased complexation energies with water molecules. For the raw chromogens, the absorption and emission band shapes have been resolved by determining vibronic factors and it turns out that a low frequency deformation strongly couples with more energetic vibrations in PODIPY, but not in BODIPY, explaining the slightly broader spectra of the former. By contrast, the inspection of the frontier molecular orbitals and density difference plots revealed that PO_2, like BF_2, plays no direct role in the chromogenic region.

The optical properties of a series of 15 new PODIPYs, substituted in various fashions, and the corresponding BODIPYs have been determined. An increase of the ground-state dipole moment was obtained in 13 out of 15 cases, hinting that the increased solubility of the PODIPYs is not limited to the two available derivatives. According to our theoretical calculations, the presence of the PO_2 group instead of the well-known fluoroborate moiety generally grants a small redshift of the AFCP energies, mainly due to the variation of the emission. The consideration of all the substitution patterns allowed us to pinpoint that the magnitude of this shift is different in aza-BODIPYs (small redshifts) and in BODIPYs (larger redshift) when replacing the fluoroborate moiety by a phosphorous group. It was also found that aza-PODIPY compounds bearing fused aromatic rings rings and/or side thiophene rings are characterized by AFCP in the near IR and are potentially interesting derivatives for *in vivo* applications, as they combine higher solubility in water and red-shifted AFCP optical signatures. This work thus provides useful insights for the future experimental developments of this promising class of fluorophores, and we are planning to extend this study to more specific asymmetric compounds similar to **17-PO$_2$**, but presenting a more pronounced charge-transfer character.

5 Acknowledgements

A. F. thank the European Research Council (ERC, Marches - 278845) for his post-doctoral grant. D. J. acknowledges the ERC and the *Région des Pays de la Loire* for financial support in the framework of a Starting Grant (Marches – 278845) and a *recrutement sur poste stratégique*, respectively. This research used resources of: 1) the GENCI-CINES/IDRIS, 2) CCIPL (*Centre de Calcul Intensif des Pays de Loire*) and 3) a local Troy cluster.

Notes and references

1 A. Loudet and K. Burgess, *Chem. Rev.*, 2007, **107**, 4891–4932.
2 G. Ulrich, R. Ziessel and A. Harriman, *Angew. Chem. Int. Ed.*, 2008, **47**, 1184–1201.
3 S. Chibani, B. Le Guennic, A. Charaf-Eddin, A. D. Laurent and D. Jacquemin, *Chem. Sci.*, 2013, **4**, 1950–1963.
4 D. Frath, J. Massue, G. Ulrich and R. Ziessel, *Angew. Chem. Int. Ed.*, 2014, **53**, 2290–2310.
5 S. L. Niu, G. Ulrich, R. Ziessel, A. Kiss, P. Renard and A. Romieu, *Org. Lett.*, 2009, **11**, 2049–2052.
6 S. L. Niu, C. Massif, G. Ulrich, R. Ziessel, P.-Y. Renard and A. Romieu, *Org. Biomol. Chem.*, 2011, **9**, 66–69.
7 S.-l. Niu, C. Massif, G. Ulrich, P.-Y. Renard, A. Romieu and R. Ziessel, *Chem. Eur. J.*, 2012, **18**, 7229–7242.
8 A. Romieu, C. Massif, S. Rihn, G. Ulrich, R. Ziessel and P.-Y. Renard, *New J. Chem.*, 2013, **37**, 1016–1027.
9 S. Zhu, J. Zhang, J. Janjanam, G. Vegesna, F.-T. Luo, A. Tiwari and H. Liu, *J. Mater. Chem. B*, 2013, **1**, 1722–1728.
10 G. Fan, L. Yang and Z. Chen, *Front. Chem. Sc. Eng.*, 2014, **8**, 405–417.
11 X.-D. Jiang, J. Zhao, D. Xi, H. Yu, J. Guan, S. Li, C.-L. Sun and L.-J. Xiao, *Chem. Eur. J*, 2015, **21**, 6079–6082.
12 A. D. Laurent, C. Adamo and D. Jacquemin, *Phys. Chem. Chem. Phys.*, 2014, **16**, 14334–14356.
13 E. Runge and E. K. U. Gross, *Phys. Rev. Lett.*, 1984, **52**, 997–1000.
14 M. E. Casida, in *Time-Dependent Density-Functional Response Theory for Molecules*, ed. D. P. Chong, World Scientific, Singapore, 1995, vol. 1, pp. 155–192.

15 C. Ullrich, *Time-Dependent Density-Functional Theory: Concepts and Applications*, Oxford University Press, New York, 2012.

16 L. Goerigk and S. Grimme, *J. Chem. Phys.*, 2010, **132**, 184103.

17 D. Jacquemin, A. Planchat, C. Adamo and B. Mennucci, *J. Chem. Theory Comput.*, 2012, **8**, 2359–2372.

18 D. Jacquemin, S. Chibani, B. Le Guennic and B. Mennucci, *J. Phys. Chem. A*, 2014, **118**, 5343–5348.

19 S. Grimme and F. Neese, *J. Chem. Phys.*, 2007, **127**, 154116.

20 D. Jacquemin, Y. Zhao, R. Valero, C. Adamo, I. Ciofini and D. G. Truhlar, *J. Chem. Theory Comput.*, 2012, **8**, 1255–1259.

21 B. Moore II and J. Autschbach, *J. Chem. Theory Comput.*, 2013, **9**, 4991–5003.

22 H. Zhekova, M. Krykunov, J. Autschbach and T. Ziegler, *J. Chem. Theory Comput.*, 2014, **10**, 3299–3307.

23 B. Le Guennic and D. Jacquemin, *Acc. Chem. Res.*, 2015, **48**, 530–537.

24 S. Chibani, A. D. Laurent, B. Le Guennic and D. Jacquemin, *J. Chem. Theory Comput.*, 2014, **10**, 4574–4582.

25 A. Charaf-Eddin, B. Le Guennic and D. Jacquemin, *RSC Adv.*, 2014, **4**, 49449–49456.

26 S. Chibani, A. D. Laurent, B. Le Guennic and D. Jacquemin, *J. Phys. Chem. A*, 2015, **119**, 5417–5425.

27 M. R. Momeni and A. Brown, *J. Chem. Theory Comput.*, 2015, **11**, 2619–2632.

28 Y. Zhao and D. G. Truhlar, *Theor. Chem. Acc.*, 2008, **120**, 215–241.

29 M. Head-Gordon, D. Maurice and M. Oumi, *Chem. Phys. Lett.*, 1995, **246**, 114–121.

30 Y. M. Rhee and M. Head-Gordon, *J. Phys. Chem. A*, 2007, **111**, 5314–5326.

31 J. Tomasi, B. Mennucci and R. Cammi, *Chem. Rev.*, 2005, **105**, 2999–3094.

32 M. Caricato, B. Mennucci, J. Tomasi, F. Ingrosso, R. Cammi, S. Corni and G. Scalmani, *J. Chem. Phys.*, 2006, **124**, 124520.

33 M. J. Frisch, G. W. Trucks, H. B. Schlegel, G. E. Scuseria, M. A. Robb, J. R. Cheeseman, G. Scalmani, V. Barone, B. Mennucci, G. A. Petersson, H. Nakatsuji, M. Caricato, X. Li, H. P. Hratchian, A. F. Izmaylov, J. Bloino, G. Zheng, J. L. Sonnenberg, M. Hada, M. Ehara, K. Toyota, R. Fukuda, J. Hasegawa, M. Ishida, T. Nakajima, Y. Honda, O. Kitao, H. Nakai, T. Vreven, J. A. Montgomery, Jr., J. E. Peralta, F. Ogliaro, M. Bearpark, J. J. Heyd, E. Brothers, K. N. Kudin, V. N. Staroverov, R. Kobayashi, J. Normand, K. Raghavachari, A. Rendell, J. C. Burant, S. S. Iyengar, J. Tomasi, M. Cossi, N. Rega, J. M. Millam, M. Klene, J. E. Knox, J. B. Cross, V. Bakken, C. Adamo, J. Jaramillo, R. Gomperts, R. E. Stratmann, O. Yazyev, A. J. Austin, R. Cammi, C. Pomelli, J. W. Ochterski, R. L. Martin, K. Morokuma, V. G. Zakrzewski, G. A. Voth, P. Salvador, J. J. Dannenberg, S. Dapprich, A. D. Daniels, O. Farkas, J. B. Foresman, J. V. Ortiz, J. Cioslowski and D. J. Fox, *Gaussian 09 Revision D.01*, 2009, Gaussian Inc. Wallingford CT.

34 S. Chibani, B. Le Guennic, A. Charaf-Eddin, O. Maury, C. Andraud and D. Jacquemin, *J. Chem. Theory Comput.*, 2012, **8**, 3303–3313.

35 B. Le Guennic, O. Maury and D. Jacquemin, *Phys. Chem. Chem. Phys.*, 2012, **14**, 157–164.

36 C. J. Cramer and D. G. Truhlar, *Acc. Chem. Res.*, 2008, **41**, 760–768.

37 A. V. Marenich, C. J. Cramer and D. G. Truhlar, *J. Phys. Chem. B*, 2009, **113**, 6378–6396.

38 Y. Shao, Z. Gan, E. Epifanovsky, A. T. Gilbert, M. Wormit, J. Kussmann, A. W. Lange, A. Behn, J. Deng, X. Feng, D. Ghosh, M. Goldey, P. R. Horn, L. D. Jacobson, I. Kaliman, R. Z. Khaliullin, T. Kuś, A. Landau, J. Liu, E. I. Proynov, Y. M. Rhee, R. M. Richard, M. A. Rohrdanz, R. P. Steele, E. J. Sundstrom, H. L. Woodcock, P. M. Zimmerman, D. Zuev, B. Albrecht, E. Alguire, B. Austin, G. J. O. Beran, Y. A. Bernard, E. Berquist, K. Brandhorst, K. B. Bravaya, S. T. Brown, D. Casanova, C.-M. Chang, Y. Chen, S. H. Chien, K. D. Closser, D. L. Crittenden, M. Diedenhofen, R. A. DiStasio, H. Do, A. D. Dutoi, R. G. Edgar, S. Fatehi, L. Fusti-Molnar, A. Ghysels, A. Golubeva-Zadorozhnaya, J. Gomes, M. W. Hanson-Heine, P. H. Harbach, A. W. Hauser, E. G. Hohenstein, Z. C. Holden, T.-C. Jagau, H. Ji, B. Kaduk, K. Khistyaev, J. Kim, J. Kim, R. A. King, P. Klunzinger, D. Kosenkov, T. Kowalczyk, C. M. Krauter, K. U. Lao, A. D. Laurent, K. V. Lawler, S. V. Levchenko, C. Y. Lin, F. Liu, E. Livshits, R. C. Lochan, A. Luenser, P. Manohar, S. F. Manzer, S.-P. Mao, N. Mardirossian, A. V. Marenich, S. A. Maurer, N. J. Mayhall, E. Neuscamman, C. M. Oana, R. Olivares-Amaya, D. P. O'Neill, J. A. Parkhill, T. M. Perrine, R. Peverati, A. Prociuk, D. R. Rehn, E. Rosta, N. J. Russ, S. M. Sharada, S. Sharma, D. W. Small, A. Sodt, T. Stein, D. Stück, Y.-C. Su, A. J. Thom, T. Tsuchimochi, V. Vanovschi, L. Vogt, O. Vydrov, T. Wang, M. A. Watson, J. Wenzel, A. White, C. F. Williams, J. Yang, S. Yeganeh, S. R. Yost, Z.-Q. You, I. Y. Zhang, X. Zhang, Y. Zhao, B. R. Brooks, G. K. Chan, D. M. Chipman, C. J. Cramer, W. A. Goddard, M. S. Gordon, W. J. Hehre, A. Klamt, H. F. Schaefer, M. W. Schmidt, C. D. Sherrill, D. G. Truhlar, A. Warshel, X. Xu, A. Aspuru-Guzik, R. Baer, A. T. Bell, N. A. Besley, J.-D. Chai, A. Dreuw, B. D. Dunietz, T. R. Furlani, S. R. Gwaltney, C.-P. Hsu, Y. Jung, J. Kong, D. S. Lambrecht, W. Liang, C. Ochsenfeld, V. A. Rassolov, L. V. Slipchenko, J. E. Subotnik, T. Van Voorhis, J. M. Herbert, A. I. Krylov, P. M. Gill and M. Head-Gordon, *Mol. Phys.*, 2015, **113**, 184–215.

39 F. Santoro, R. Improta, A. Lami, J. Bloino and V. Barone, *J. Chem. Phys.*, 2007, **126**, 084509. FCClasses is available at http://www.pi.iccom.cnr.it/fcclasses [Accessed Oct. 2015]..

40 F. Santoro, R. Improta, A. Lami, J. Bloino and V. Barone, *J. Chem. Phys.*, 2007, **126**, 184102.

41 F. Santoro, A. Lami, R. Improta, J. Bloino and V. Barone, *J. Chem. Phys.*, 2008, **128**, 224311.

42 F. J. Avila Ferrer, J. Cerezo, E. Stendardo, R. Improta and F. Santoro, *J. Chem. Theory Comput.*, 2013, **9**, 2072–2082.

43 A. B. Nepomnyashchii and A. J. Bard, *Acc. Chem. Res.*, 2012, **45**, 1844–1853.

44 H. Lu, J. Mack, Y. Yang and Z. Shen, *Chem. Soc. Rev.*, 2014, **43**, 4778–4823.

45 We have tested the complexation of one water molecule with the nitro group for **1-PO$_2$** and found a smaller complexation energy than with the PO$_2$ ligand (4.32 kcal.mol^{-1}).

46 A. Gorman, J. Killoran, C. O'Shea, T. Kenna, W. Gallagher and D. F. O'Shea, *J. Am. Chem. Soc.*, 2004, **126**, 10619–10631.

47 P.-A. Bouit, K. Kamada, P. Feneyrou, G. Berginc, L. Toupet, O. Maury and C. Andraud, *Adv. Mater.*, 2009, **21**, 1151–1154.

48 X. Zhang, H. Yu and Y. Xiao, *J. Org. Chem.*, 2012, **77**, 669–673.

49 R. Gresser, M. Hummert, H. Hartmann, K. Leo and M. Riede, *Chem. Eur. J.*, 2011, **17**, 2939–2947.

50 W. L. Zhao and E. M. Carreira, *Chem. Eur. J.*, 2006, **12**, 7254–7263.

51 Y. Kubota, H. Hara, S. Tanaka, K. Funabiki and M. Matsui, *Org. Lett.*, 2011, **13**, 6544–6547.

52 V. Leen, T. Leemans, N.Boens and W. Dehaen, *Eur. J. Org. Chem.*, 2011, 4386–4396.

53 C. Yu, Y. Xu, L. Jiao, J. Zhou, Z. Wang and E. Hao, *Chem. Eur. J*, 2012, **18**, 6437–6442.

54 E. Deniz, G. C. Isbasar, O. A. Bozdemir, L. T. Yildirim, A. Siemiarczuck and E. U. Akkaya, *Org. Lett.*, 2008, **10**, 3401–3403.

55 S. Niu, G. Ulrich, P. Retailleau and R. Ziessel, *Org. Lett.*, 2011, **13**, 4996–4999.

Graphical Abstract

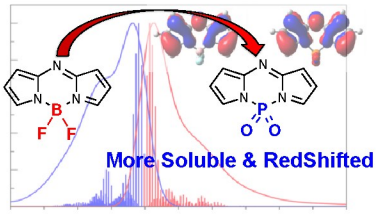

What are the differences between BODIPYs and PODIPYs ?